PACS numbers: 42.81.Dpl 42.65.Dr
DOI: 10.1070/QE2000v030n06ABEH001765

Ultimate intensities of light in silica fibres: stimulated Raman scattering as the main thermal source of optical destruction

A S Biryukov, E M Dianov

Abstract. It is shown that, under certain conditions, the intensity of light in silica fibres is mainly limited by stimulated Raman scattering. An estimate is made of the threshold intensity that leads to irreversible destruction of the fibre due to overheating. The dependence of the threshold intensity on physicochemical properties of the material and the geometric dimensions of the fibre core is determined.

The specific phenomenon of destruction of the fibre core during propagation of intense radiation has been under investigation for more than decade [1 – 5]. The specific feature of this phenomenon is that the defects originate from artifical inhomogeneities, such as a contaminated output face or a locally heated part of the fibre, and then propagate in the core as a regular chain of oxygen-containing cavities towards the radiation source. The propagation speed of destructions increased with increasing intensity of light I, and for $I > 5$ MW cm^{-2} it was ~ 1 m s^{-1}.

In the same investigations, the thermal nature of this destruction process was established. For example, Kashyap [1] substantiated this claim by measuring absorption of radiation of a wavelength of 1.064 μm in a single-mode fibre. An arbitrary one-meter-long stretch of this fibre was heated up to temperature of 1100 °C. The measured absorption was weak at temperatures up to ~ 1050 °C, but then dramatically increased, reaching a value of approximately 2×10^3 dB km^{-1} at $T \approx 1000$ °C, and grew even further. Obviously, for some intensity of light, the rate of light energy absorption became comparable to that of the heat dissipation, and the further self-accelerating process of absorption and heating resulted in destruction of the fibre.

Hand et al. [2] explained the propagation of destructions towards the radiation coupled to the fibre by the action of a thermal shock wave. According to the authors, this shock wave appears upon absorption of light by the artificial inhomogeneity, which leads to the local heating, formation of a focusing thermal lens, and a further increase in absorption and temperature, etc. As a result, a very small volume (of the order of 1 μm^3) is heated up to temperatures of about several thousand degrees. Such temperatures are sufficient not only to melt a silica glass, but also to sublimate it (the process is accompanied by partial decomposition of SiO_2 into SiO and oxygen), and even to produce a plasma. The radiation that is still coupled into the fibre is now completely absorbed near the locally overheated volume. About 95% of the absorbed radiation energy contributes to further heating of the volume, with the rest re-emitted as radiation with the black-body-like spectrum. This process results in expansion of the overheated volume in the direction of the incoming injected radiation. The observed periodicity of the created destruction cavities is explained by the instability of the thermal wave, which, in turn, is caused by the instability of the effective diameter of the radiation mode [2].

However, the authors [1 – 5] have not discussed the possibility of a similar spontaneous phenomenon, i.e., the appearance of destructions in an ideal fibre that does not contain distinct inhomogeneities of the type discussed above. Nevertheless, this is a fully legitimate question. For example, it is closely related to the problem of creation of powerful fibre lasers. Extensive studies in this field has already resulted in the development of a cw single-mode fibre laser with the record output power of 35 W [6]. This laser consists of a fibre with a core doped with 1.5 % of Yb, which is placed inside a resonator and is pumped by LEDs at the wavelength 915 nm.

Taking the value of the effective cross section of the mode into account, the attained output power corresponds to the maximum light intensity of ~ 140 MW cm^{-2} at the fibre core, which is much greater than the light intensities used in Refs [1 – 5]. On the other hand, it was noted (e.g., in Ref. [7]) that the real thresholds for optical destruction of silica fibres correspond to light intensities of more than 10 GW cm^{-2}, which, however, is still much lower than the threshold of electrical breakdown of a silica glass. This means that, for high intensities of light, even in 'ideal' fibres the heat release can be great enough to cause their destruction.

Like the authors of Refs [1 – 5], we consider thermal effects to be the cause of optical destruction of the fibre core. In this connection, we show in this paper that stimulated Raman scattering (SRS) is the most probable source of heat that can trigger the chain of processes leading to optical destruction. In other words, the SRS process may create local thermal singularities, in an 'ideal' fibre, which are analogous to the artificial inhomogeneities discussed in Refs [1 – 5].

Below we will consider the case of high radiation intensities that are much greater than the destruction thresholds of Refs [1 – 5], i.e., greater than 3 MW cm^{-2}. In this situation, the nonlinear effects in optical fibres play the leading role. At present, a number of nonlinear optical phenomena are known, which are determined by the second and the higher powers of the electric component of the light fields. For example, these include generation of harmonics, the non-

A S Biryukov, E M Dianov Scientific Centre of Fibre Optics, Institute of General Physics, Russian Academy of Sciences, ul. Vavilova 38, 117942 Moscow, Russia

Received 25 June 1999
Kvantovaya Elektronika **30** (6) 559 – 564 (2000)
Translated by I V Bargatin, edited by M N Sapozhnikov

linear Kerr effect, stimulated Raman scattering (SRS), stimulated Brillouin scattering (SBS), various parametric processes, etc. However, only some of these processes, including SRS and SBS, are accompanied by heating of the matter.

As for SBS and stimulated Rayleigh scattering, the frequency shift of the scattered wave in these processes is rather small and so is the fraction of the energy of the electromagnetic field that is converted to heat in each scattering event. In contrast, the SRS process is accompanied by much greater heat release. In this case, over 5% of the radiation energy coupled to a silica fibre can convert to heat in each scattering event (for the light wavelength greater than 1 μm). For these reasons, it is SRS that may limit the intensity of light passing through an 'ideal' fibre.

We will now try to determine this ultimate intensity and other factors that may lead to overheating of an optical fibre.

Because the excitation threshold of SBS in silica glass is much lower than that of SRS, we will assume in the study of the role of SRS in thermal fibre destruction that the SBS process is suppressed. (Otherwise, because the scattered radiation and radiation coupled to a fibre are counterpropagating, the SBS process will result in reflection of the coupled radiation, thereby prohibiting injection of light into the fibre.) The methods for suppression of SBS are well known and are based on the narrowness of the SBS-amplification spectral linewidth (which is ~ 100 MHz in a silica glass [8]). Therefore, the efficiency of excitation of SBS can be made much lower than that of SRS by using injected radiation with a wider spectrum.

Consideration of overheating of a fibre requires the use of a set of equations describing SRS and the heat conduction equations.

The equations describing SRS can be written, for example, in the form [9]:

$$\frac{\mathrm{d}I_\mathrm{p}}{\mathrm{d}z} = -I_\mathrm{p}\left(\alpha_\mathrm{p} + gI_{\mathrm{s},1}\frac{v_\mathrm{p}}{v_{\mathrm{s},1}}\right),$$

$$\frac{\mathrm{d}I_{\mathrm{s},1}}{\mathrm{d}z} = I_{\mathrm{s},1}\left(-\alpha_{\mathrm{s},1} - gI_{\mathrm{s},2}\frac{v_{\mathrm{s},1}}{v_{\mathrm{s},2}} + gI_\mathrm{p}\right),$$

$$\cdots\cdots\cdots\cdots\cdots\cdots\cdots\cdots\cdots\cdots\cdots\cdots\cdots\cdots\cdots\cdots\cdots\cdots \quad (1)$$

$$\frac{\mathrm{d}I_{\mathrm{s},n-1}}{\mathrm{d}z} = I_{\mathrm{s},n-1}\left(-\alpha_{\mathrm{s},n-1} - gI_{\mathrm{s},n}\frac{v_{\mathrm{s},n-1}}{v_{\mathrm{s},n}} + gI_{\mathrm{s},n-2}\right),$$

$$\frac{\mathrm{d}I_{\mathrm{s},n}}{\mathrm{d}z} = I_{\mathrm{s},n}(-\alpha_{\mathrm{s},n} + gI_{\mathrm{s},n-1}),$$

Here, I_p is the intensity of light of frequency v_p coupled to a fibre (in the following, we will refer to it as pumping radiation); $I_{\mathrm{s},i}$ is the intensity of the Stokes components with frequencies $v_{\mathrm{s},i}$ $(i = 1, \ldots, n)$; n is the total number of these components; $\alpha_\mathrm{p} = \alpha_\mathrm{p}(v)$ and $\alpha_{\mathrm{s},i} = \alpha_{\mathrm{s},i}(v)$ are the frequency-dependent coefficients of linear attenuation in the fibre; and g is the SBS gain.

The transverse intensity distribution of the fundamental fibre mode can be well approximated by the Gaussian function [8]. Therefore, we set in Eqn (1) $I_\mathrm{p} = I_\mathrm{p}(z,0)\exp(-r^2/w^2)$ and $I_{\mathrm{s},i} = I_{\mathrm{s},i}(z,0)\exp(-r^2/w^2)$, where w is the effective radius of the fundamental mode; $I_\mathrm{p}(z,0)$ and $I_{\mathrm{s},i}(z,0)$ are the corresponding intensities on the fibre axis. In multimode step optical fibres whose core radius is much larger than the wavelength, the intensity distribution can be taken to be virtually uniform across the core. In other cases, specification of the corresponding radial distributions I_p and $I_{\mathrm{s},i}$ is necessary.

For simplicity, we will consider the heat conduction equation in the quasistationary approximation. This approximation is valid for cw radiation or sufficiently long pulses propagating in a fibre whose duration exceeds the characteristic time of radial heat transfer $\tau = R^2 c\rho/\lambda$, where R is the radius of the fibre core; c, ρ, and λ are, respectively, the specific heat, the density, and the heat conductivity of a silica glass. All other thermal processes take place at much shorter times. For example, the time it takes to dissipate the energy of the SBS-induced vibrational excitation of the medium typically does not exceed $\sim 10^{-10}$ s, whereas $\tau \approx 10$ μs for a silica fibre with the radius $R \approx 4$ μm. For shorter pulses, the nonstationary heat conduction equation should be used.

The heat conduction equation takes the following form in the quasistationary approximation

$$\lambda\Delta T = Q\ . \quad (2)$$

Here, $Q = Q(r,z)$ is the heat source, which is determined by the power density of the heat production rate and which equals the sum of the right hand sides of Eqns (1):

$$Q = -\left\{I_\mathrm{p}(z,0)\left[\alpha_\mathrm{p} + g\frac{\Delta v}{v_{\mathrm{s},1}}I_{\mathrm{s},1}(z,0)\exp\left(-\frac{r^2}{w^2}\right)\right] + \sum_{i=1}^{n} I_{\mathrm{s},i}(z,0)\left[\alpha_{\mathrm{s},i} + g\frac{\Delta v}{v_{\mathrm{s},i+1}}I_{\mathrm{s},i+1}(z,0)\exp\left(-\frac{r^2}{w^2}\right)\right]\right\} \times \exp\left(-\frac{r^2}{w^2}\right),$$

where $\Delta v = v_\mathrm{p} - v_{\mathrm{s},1} = v_{\mathrm{s},i} - v_{\mathrm{s},i+1}$ (for a silica glass, $\Delta v \approx 440$ cm^{-1} [8]).

The use of the linear heat conduction Eqn (2) for our purposes is well justified, since the variance of the heat conductivity of a silica glass is less than $\sim 50\%$ over the considered temperature range (from room temperature to ~ 1000 °C). On the other hand, the maximal radial temperature gradient in the fibre does not exceed -20 K μm^{-1}, as we show below. Because $\mathrm{d}n/\mathrm{d}T \approx 10^{-5}$ for the refractive index of a silica glass, this temperature gradient corresponds to $|\mathrm{d}n/\mathrm{d}r| \leqslant 3 \times 10^{-4}$ μm^{-1}. Thus, the focusing effect of the thermal lens in the fibre is hardly noticeable before the start of the optical destruction process.

The system of Eqns (1) is nonlinear and, therefore, it cannot be solved analytically in the general case. However, we have both numerical methods and some reliable approximate models at our disposal.

First, we note that, in a good approximation, we can neglect the longitudinal temperature gradient with respect to the radial one. This is explained by the substantial difference between the geometric scales of the heat conduction process in the two directions (the radius of a fibre is much smaller than its longitudinal dimension). Therefore, in the considered approximate model, the temperature distribution is determined by the action of the longitudinally distributed heat source Q and the radial heat conduction process.

Second, it follows from Eqn (1) that because of the nonlinearity the maximum of every subsequent Stokes compo-nent is located farther along the fibre axis z than the preceding one. This also means that the maxima of the temperature distribution along the fibre, according to Eqn (3), correspond to the locations where one of the Stokes

components is transformed into another most efficiently. The intensity of each appearing Stokes component is lower than those of the already existing components because of the heat release; therefore the location where $Q(z)$ reaches its maximum corresponds to the moment of appearance of the first Stokes component of the pumping radiation.

To estimate the maximum heating, we can therefore restrict ourselves to the coordinates z that correspond to the maximum of the intensity of the first Stokes component. We can also omit in (1) all equations corresponding to the higher Stokes components and in Eqn (3) retain only the terms related to the appearance of the first Stokes component. Thus, it is the appearance of the first Stokes component that leads to formation of the local thermal singularity in an 'ideal' fibre; this singularity is analogous to the artificial inhomogeneities discussed in Refs [1–5].

Third, in addition to the approximations already made, we neglect the linear terms with respect to the nonlinear terms in Eqns (1) and (3), which is a common practice during analysis of SRS [8].

Taking into account the mentioned approximations, the system of Eqns (1)–(3) takes a simple form

$$\begin{aligned}
&\frac{1}{r}\frac{\partial}{\partial r}\, r\,\frac{\partial T}{\partial r} = \frac{Q}{\lambda}\,,\\
&\frac{\mathrm{d}I_\mathrm{p}}{\mathrm{d}z} = -gI_\mathrm{p}I_\mathrm{s}\,\frac{v_\mathrm{p}}{v_\mathrm{s}}\,,\\
&\frac{\mathrm{d}I_\mathrm{s}}{\mathrm{d}z} = gI_\mathrm{p}I_\mathrm{s}\,,\\
&Q = -g\,\frac{\Delta v}{v_\mathrm{s}}\,I_\mathrm{p}I_\mathrm{s}\,.
\end{aligned} \tag{4}$$

Note here that, in the form they are written, the equation systems (4) and (1) have only restricted applicability. Namely, these SRS-amplifier equations can be solved only when there is already a certain number of photons of the Stokes component in the coupled fibre mode. Conversely, if the coupled radiation consists of the pumping component only, the two equation systems cannot be formally solved. The problem of development of the SRS processes that are triggered by spontaneous noise is not currently fully clarified. Therefore, for the sake of determinacy, we assumed that I_s in Eqns (1), (3), and (4) stands for $I_\mathrm{s}+S$, where S is the intensity that corresponds to the presence of at least one photon of the Stokes component wavelength in the coupled mode (see, e.g., Ref. [10]). We chose the particular values of S in accordance with the estimates and recommendations of Refs [8, 11].

We assumed that the gain g is independent of the temperature, although some unknown dependence is probably present. We then solve Eqn (4) first for the intensities $I_\mathrm{p}(z,r)$ and $I_\mathrm{s}(z,r)$, and then for the distribution of the heat release $Q(z,r)$,

$$\begin{aligned}
&I_\mathrm{p} = \left(I_{\mathrm{p}0} + S\,\frac{v_\mathrm{p}}{v_\mathrm{s}}\right)\frac{1}{A}\,,\\
&I_\mathrm{s} = S\left\{\exp\left[gz\left(I_{\mathrm{p}0} + S\,\frac{v_\mathrm{p}}{v_\mathrm{s}}\right)\right] - 1\right\}\frac{1}{A}\,,\\
&A = 1 + Sv_\mathrm{p}\exp\left[gz\left(I_{\mathrm{p}0} + S\,\frac{v_\mathrm{p}}{v_\mathrm{s}}\right)\right]\frac{1}{I_{\mathrm{p}0}v_\mathrm{s}}\,,
\end{aligned} \tag{5}$$

where $I_{\mathrm{p}0}$ is the radial distribution of the pumping intensity at the entry surface of the fibre ($z=0$).

Using Eqn (5), we find from Eqn (4)

$$\begin{aligned}
Q(z,r) = &-gS\Delta v\left(I_{\mathrm{p}0} + S\,\frac{v_\mathrm{p}}{v_\mathrm{s}}\right)\\
&\times\left\{\exp\left[gz\left(I_{\mathrm{p}0} + S\,\frac{v_\mathrm{p}}{v_\mathrm{s}}\right)\right] - 1\right\}\frac{1}{v_\mathrm{s}A^2}\,.
\end{aligned} \tag{6}$$

Next, we find approximately the coordinate z where the function $Q(z,r)$ reaches its maximal value

$$z_\mathrm{max} \approx \left[\ln\left(\frac{I_{\mathrm{p}0}v_\mathrm{s}}{Sv_\mathrm{p}}\right)\right]\frac{1}{gI_{\mathrm{p}0}} \tag{7}$$

and the maximal value itself

$$Q_\mathrm{max} \approx -\frac{1}{4}\,gI_{\mathrm{p}0}^2\,\frac{\Delta v}{v_\mathrm{p}}\,. \tag{8}$$

One can see from the approximate solutions (7) and (8) that the location of the maximal heat release z_max only weakly depends on the value of the ill-defined quantity S. For the considered radiation intensities, the variance of z_max lies within $\sim 20\%$ even when S varies over two orders of magnitude.

If one uses Eqn (6) for the heat source Q, the resulting expression for the temperature distribution will be very cumbersome and of little practical value. Therefore, we will restrict ourselves to merely finding the analytical expression for the radial temperature distribution at the cross section that corresponds to the coordinate $z = z_\mathrm{max}$. Setting in Eqn (4) $Q = Q_\mathrm{max}$ and using the radial distribution of the radiation intensity, we find

$$T(z_\mathrm{max},r) = \frac{aw^2}{8\lambda}\,\mathrm{Ei}\left(-\frac{2\mathrm{r}^2}{w^2}\right) + \mathrm{C}_1\ln\mathrm{r} + \mathrm{C}_2\,, \tag{9}$$

where $a = gI_{\mathrm{p}0}^2(0,0)\delta v/(4v_\mathrm{p})$, and the integration constants C_1, C_2 are chosen to comply with the boundary conditions.

In order to specify these boundary conditions, we will consider a typical example of a single-mode silica fibre with polymer coating. We will take its core radius to be R_1 and the radius of its cladding to be $R_2 = 62.5$ μm. The thickness of the polymer coating then equals $R_3 - R_2$, where R_3 is the total radius of the fibre cross section. In accordance with the given structure of the fibre, the solutions of Eqn (9) take the following form for the three layers of the fibre

$$\begin{aligned}
&T_1 = \frac{aw^2}{8\lambda_1}\sum_{k=1}^{\infty}\left(-\frac{2r^2}{w^2}\right)^k\frac{1}{k^*k!} + G \quad (0 \leqslant r \leqslant R_1)\,,\\
&T_2 = \left(B + \frac{aw^2}{4\lambda_2}\right)\ln r + \frac{aw^2}{8\lambda_2}\sum_{k=1}^{\infty}\left(-\frac{2r^2}{w^2}\right)^k\frac{1}{k^*k!} + C\\
&(R_1 \leqslant r \leqslant R_2)\,,\\
&T_3 = D\ln r + E \quad (R_2 \leqslant r \leqslant R_3)\,.
\end{aligned} \tag{10}$$

Here T_1, T_2, and T_3 are, respectively, the temperatures of the core, the cladding, and the polymer coating; G, B, C, D, and E are the integration constants for the corresponding fibre layers, which replace C_1 and C_2 of Eqn (9); λ_1, λ_2, λ_3 are the heat conductivity coefficients of the three layers. Eqn (10) accounts for the fact that there is no radiation

propagating inside the coating; the core integration constant was taken to be $aw^2(4\lambda_1)^{-1}$ in order to preclude the logarithmic divergence of the solution at $r = 0$.

Taking into account the described fibre structure, we have the following expressions for the boundary conditions of the heat conduction equation

$$T_1(R_1) = T_2(R_1)\,, \quad T_2(R_2) = T_3(R_2)\,,$$
$$\lambda_1 \frac{\partial T_1}{\partial r}\bigg|_{R_1} = \lambda_2 \frac{\partial T_2}{\partial r}\bigg|_{R_1}\,, \quad \lambda_2 \frac{\partial T_2}{\partial r}\bigg|_{R_2} = \lambda_3 \frac{\partial T_3}{\partial r}\bigg|_{R_2}\,, \qquad (11)$$
$$\lambda_3 \frac{\partial T_3}{\partial r}\bigg|_{R_3} = -h[T_3(R_3) - T_0]\,,$$

where the coefficient h describes the heat exchange between the outer layer of the fibre and environment, which we assume to be at temperature T_0.

Next, we set $w \approx R_1$ [8] and eliminate the integration constants from Eqn (10) with the help of Eqn (11):

$$T_1 = \Phi + \frac{aR_1^2}{8\lambda_2}\sum_{k=1}^{\infty}\left[\left(1 - \frac{\lambda_2}{\lambda_1}\right)2^k - \left(\frac{2R_2^2}{R_1^2}\right)^k + \frac{\lambda_2}{\lambda_1}\left(\frac{2r^2}{R_1^2}\right)^k\right]\frac{(-1)^k}{k^*k!}\,,$$
$$T_2 = \Phi + \frac{aR_1^2}{8\lambda_2}\sum_{k=1}^{\infty}\left[\left(\frac{2r^2}{R_1^2}\right)^k - \left(\frac{2R_2^2}{R_1^2}\right)^k\right]\frac{(-1)^k}{k^*k!}\,, \qquad (12)$$
$$T_3 = \Phi + \frac{aR_1^2}{4\lambda_3}\left[1 - \exp\left(-\frac{2R_2^2}{R_1^2}\right)\right]\ln\frac{R_2}{r}\,,$$
$$\Phi = T_0 + \frac{aR_1^2}{4\lambda_3}\left[1 - \exp\left(-\frac{2R_2^2}{R_1^2}\right)\right]\left(\ln\frac{R_3}{R_2} + \frac{\lambda_3}{hR_3}\right)\,.$$

We used the following parameter values for our calculations: $R_1 = 4$ μm, $R_2 = 62.5$ μm, $R_3 = 110$ μm; $\lambda_1 \approx \lambda_2 = 1.46 \times 10^{-2}$ W cm^{-1} deg^{-1} [12], $\lambda_3 = 1.9 \times 10^{-3}$W cm^{-1} deg^{-1} for polymethylacrylate [13]; $h \approx 1.7 \times 10^{-2}$ W cm^{-2} deg^{-1} [14]. We also assumed that the fibre was pumped by a neodymium laser at the wavelength 1.064 μm ($\nu_p \approx 9400$ cm^{-1}); for the SRS amplification coefficient, we used the corresponding value for a silica glass $g = 10^{-11}$ cm W^{-1} [8].

In order to substantiate the use of the approximate model Eqns (4)–(12) for the below estimates, we first calculated the distribution of the heat release Q over the fibre axis employing both the general Eqns (1), (3) and the approximate Eqns (4)–(12). We used the dependence of the linear attenuation coefficient on the radiation wavelength as given, for example, in Ref. [15].

Fig. 1 shows the maximal heat release $Q(0, z_{max})$ and the coordinate z_{max} as functions of the pumping intensity, at the moment of the most efficient conversion of the pumping radiation to the first Stokes component. According to the numerical solution of Eqn (1), (3), for $I_{p0} = 100$ MW cm^{-2}, one has $Q(0, z_{max}) = 1.25$ kW cm^{-3} and z_{max} =190 m, whereas calculation according to the approximate formulas (7), (8) gives 1.17 kW cm^{-2} and 207 m, respectively.

The rate of the SRS process grows with increasing pumping intensity, so that the first Stokes component shows up nearer to the fibre entry surface. Note that an increase of the intensity results in decreased contribution of the linear losses into the maximal heat release. The accuracy of the approximate model then improves, and the deviation of the approximate results for Q_{max} and z_{max} [calculated according to Eqns (7) and (8)] from the exact numerical values lessens. On these grounds, we believe that for high pumping intensities the radial temperature distributions obtained with the help of formulas (12) are close to the exact ones.

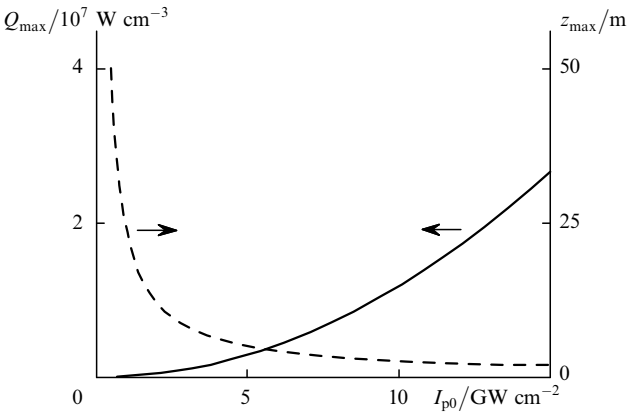

Figure 1. The maximal heat release $Q(0, z_{max})$ (solid curve) and the position of the maximum on the fibre axis (dashed curve) as functions of the pumping intensity.

In our opinion, the above results show that the claims of the authors of Ref. [6] about possible optical destruction and strong nonlinear effects at intensities greater than 100 MW cm^{-2}, are exaggerated, at least regarding the destruction process. For example, the intensity 300 MW cm^{-2} (which corresponds to the output power ~ 150 W for $R_1 = 4$ μm) excites the SRS process inside a section of the fibre that is more than 60 meters long. Therefore, shorter fibre stretches have a sufficient intensity margin over the intensity realised in Ref. [6] for a fibre stretch 50 m long.

Fig. 2 shows the radial temperature distributions for much greater pump intensities: 14 and 20 GW cm^{-2}. Each curve refers to the corresponding cross section of the maximal heat release, as defined by the emergence of the first Stokes component. The longitudinal coordinates of these cross sections were found to be approximately ~ 1.8 m and 1.3 m, respectively. One can see from the figure that the intense heat release of the SRS process may raise the temperature on the fibre axis beyond the above-mentioned critical level ~ 1100 °C if the pumping intensity I_p exceeds 20 GW cm^{-2}. The triggered self-accelerating process of absorption and heating then results in destruction of the fibre core.

In the above model, we did not take into account an additional factor that should accelerate the overheating, namely, the self-focusing of the wave towards the fibre axis. This factor slightly lowers the threshold of the optical destruction: If this factor is taken into account, the critical intensity will probably approach the value 10 GW cm^{-2} given in Ref. [7]. Therefore the maximal power that can be transmitted through a lengthy fibre without destroying it does not exceed ~ 5 kW (including the reduction due to self-focusing). The self-focusing effects make the problem considerably more complicated since one has also to calculate the radial distribution of the radiation intensity, including the temperature dependence of the refractive index.

Fig. 2 shows that injection of high radiation intensities $I > 15$ GW cm^{-2} should strongly degrade the polymer coating at the zone of maximal heat release. This degradation,

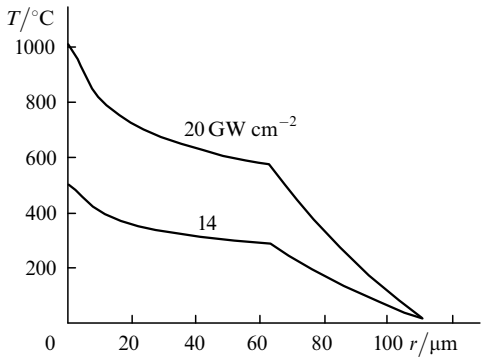

Figure 2. The calculated radial temperature distribution in the cross sections of maximal heat release for two pumping intensities: 14 GW cm^{-2} and 20 GW cm^{-2}.

which may start even before destruction of the core, will result in complete loss of strength of the fibre. Assuming that degradation of polymers, on average, starts at temperatures about ~ 300 °C, we find that the corresponding critical power does not exceed 4 – 5 kW, which is comparable to the threshold of the core destruction. The uncertainty in the above estimate is due to the low accuracy of the calculated values of T_3, which, in turn, is related to the low precision of the value of the heat-exchange coefficient h used in Eqn (12).

Finally, we will say a few words about the thermal effect of SRS in fibres with phosphorus-doped cores. Such fibres are now being extensively studied for applications in fibre SRS lasers and amplifiers [16]. In addition to the SRS shift $\Delta v \approx 440$ cm^{-1} caused by a silica glass network, these fibres feature a much larger SRS frequency shift $\Delta v \approx 1330$ cm^{-1} caused by the presence of P_2O_5 in a silica glass (see, e.g., Ref. [17]). Seemingly, the threefold increase of the SRS frequency shift with respect to the pure SiO_2 in this case must lead to greater heat release, acceleration of the above-described processes, and lowering of the optical destruction threshold.

However, this is not generally the case. The zones of maximal heat release that correspond to excitation of the Stokes components with the frequency shift 440 cm^{-1} and 1330 cm^{-1} are typically localised in different fibre cross sections, so that their heating action is not additive. This is explained, on the one hand, by the almost 3.5-fold difference between the SRS cross sections of P_2O_5 and SiO_2 [18]. On the other hand, the content of the dopant P_2O_5 in a silica glass should be sufficiently low to avoid unacceptable optical loss in the fibre.

The total excitation rate of the SRS with the frequency shift 1330 cm^{-1} in doped glass is determined by both the discussed factors. Given the experimentally determined optimal value $\sim 11 - 13\%$ of the molecular content of P_2O_5 in glass [19], this excitation rate is at least two times less than the excitation rate of SRS with the frequency shift 440 cm^{-1}.

The energy of the pumping radiation is thus redistributed into excitation of different Stokes components corresponding to different frequency shifts. As a result, the actual threshold of optical destruction in phosphorus-doped silica glass is even greater than the one in pure SiO_2.

References

1. Kashyap R Proc. Int. Conf. Laser'87 Lake Tahoe, NV, USA (McLean, VA, STS Press, 1987) pp. 859-866
2. Hand D P, Russell P S J. Opt. Lett. **13** 767 (1988)
3. Kashyap R, Blow K J. Electron. Lett. **24** 47 (1988)
4. Driscoll T J, Calo J M, Lawandy N M Opt. Lett. **16** 1046 (1991)
5. Dianov E M, Mashinsky V M, Myzina V A et al. Sov. Lightwave Comm. **2** 293 (1992)
6. Muendel M, Engstrom B, Kea D et al. Postdeadline Papers Intern. Conf. on Lasers and Electro-Optics (CLEO'97) (Baltimore, MD, 1997, CPD30)
7. Stolen R H, in: Optical Fibre Telecommunications (New York, Acad. Press, 1979) p. 145
8. Agrawal G Nonlinear Fibre Optics (Berkeley, Academic Press, 1989)
9. Nakashima T, Seikai S, Nakazawa M J. Lightwave Technol. **4** 569 (1986)
10. Auyeung J, Yariv A IEEE J. Quantum. Electron. **14** 347 (1978)
11. Smith R G Appl. Opt. **11** 2489 (1972)
12. Tablitsy Fizicheskikh Velichin. Spravochnik [Tables of Physical Quantities. Reference Book] (Moscow, Atomizdat, 1976)
13. Entsiklopediya Polimerov [Encyclopaedia of Polymers] (Moscow, Sovetskaya Entsiklopediya, 1977, vol. 3) p. 599
14. Paek U C, Kurkjian C R J. Am. Ceram. Soc. **58** 330 (1975)
15. Belov A V, Gur'yanov A N, Gusovskii D D Sov. J. Quantum Electron. **17** 207 (1990) [Kvantovaya Elektronika **17** 266 (1990)]
16. Dianov E M, Grekov M V, Bufetov I A et al. Electron. Lett. **33** 1542 (1997)
17. Grigoryants V V, Davydov B L, Zhabotinskii M E et al. Opt. Quantum Electron. **9** 351 (1977)
18. Galeener F L, Mikkelsen J C Jr., Geils H R, Mosby W J. Appl. Phys. Lett. **32** 34 (1978)
19. Dianov E M, Bufetov I A, Bubnov M M et al. (to be published)